Macromolecules

Article

pubs.acs.org/Macromolecules

Effect of Fluorination on Molecular Orientation of Conjugated Polymers in High Performance Field-Effect Transistors

Andong Zhang,[†,⊥] Chengyi Xiao,[†] Yang Wu,[‡] Cheng Li,[*,†] Yunjing Ji,[†] Lin Li,[§] Wenping Hu,[†] Zhaohui Wang,[*,†] Wei Ma,[*,‡] and Weiwei Li[*,†]

[†]Beijing National Laboratory for Molecular Sciences, CAS Key Laboratory of Organic Solids, Institute of Chemistry, Chinese Academy of Sciences, Beijing, 10090, China

[‡]State Key Laboratory for Mechanical Behavior of Materials, Xi'an Jiaotong University, Xi'an 710049, PR China

[§]College of Chemistry, Beijing Normal University, Beijing, 100875, PR China

[⊥]University of Chinese Academy of Sciences, Beijing 100049, PR China

Supporting Information

ABSTRACT: Fluorinated conjugated polymers have been widely used in high performance polymer solar cells, but they showed limited application in field-effect transistors (FETs). In this paper, we focus on the influence of fluorine atoms upon charge transport of conjugated polymers in FET devices. Two series of conjugated polymers without or with fluorine atoms were designed and applied into FETs. Nonfluorinated conjugated polymers show high hole mobilties up to 11.16 $cm^2\ V^{-1}\ s^{-1}$, while fluorinated polymers exhibit low hole mobilities below 1.80 $cm^2\ V^{-1}\ s^{-1}$. Further investigation by differential scanning calorimetry (DSC) and 2D grazing-incidence wide-angle X-ray scattering (2D-GIWAXS) reveal that fluorinated conjugated polymers show low crystallinity and "face-on" orientation in thin films, explaining their poor hole mobilities in FET devices. Our results clearly show how the chemical structures influence the charge transport properties, which can be used to design new conjugated polymers toward high performance FETs.

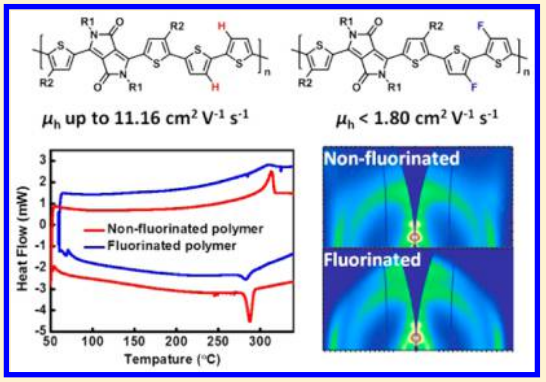

1. INTRODUCTION

Developing high performance organic field-effect transistors (OFETs) has become one of the important goals for chemists and material scientists owing to their promising application in flexible and lightweight electronic devices.[1] To accomplish this goal, conjugated polymers are particularly preferred since they can be fabricated via solution-processed techniques, such as roll-to-roll printing, facilitating large area, and low cost transistor devices.[2−8] The incredible richness of chemical structures also allow the chemists to developing numerous conjugated polymers, resulting in the high hole,[9−13] electron[2,7,14−20] and ambipolar mobilities[21−23] exceeding 1 $cm^2\ V^{-1}\ s^{-1}$ nowadays, which is beyond those of typical amorphous silicon-based FETs (0.5−1 $cm^2\ V^{-1}\ s^{-1}$). The outstanding performance provides the opportunity to deeply understand the relationship between chemical structures of conjugated polymers and charge transport, which will guide the designation of new conjugated polymers toward flexible OFET devices for industrial application.

The intrinsic field-effect mobility of an OFET device mainly depends on the molecular structure and the intermolecular packing, which is rather complicate in conjugated polymers. The delocalized π-systems in conjugated polymers are generally responsible for the charge transport, which are strongly influenced by the semicrystal nature of the polymers. The $\pi-\pi$ interaction and other noncovalent force can help conjugated polymers to form ordered and crystalline region, while the long conjugated backbone and flexible alkyl side chains cause the disorder region. Interestingly, although most of researches reveal that highly crystalline conjugated polymers provide high mobilities,[24−26] some amorphous conjugated polymers were also found to have high mobilities.[27−31] In another aspect, the charge carriers transport along the direction that is parallel to the substrate, indicating that the $\pi-\pi$ stacking ordering parallel to the substrate (so-called "edge-on" configuration) has higher mobility.[20,32−34] However, it also reported that some conjugated polymers with "face-on" orientation can also provide similar high mobilities.[35−38] The above-mentioned issues, including the impact of the crystalline nature and the backbone orientation of conjugated polymers on charge transport of polymers, are required to be further investigated.

In this work, we are interested in finding how the chemical structures influence on the microstructure of the conjugated

Received: July 6, 2016
Revised: August 26, 2016

DOI: 10.1021/acs.macromol.6b01446
Macromolecules XXXX, XXX, XXX−XXX

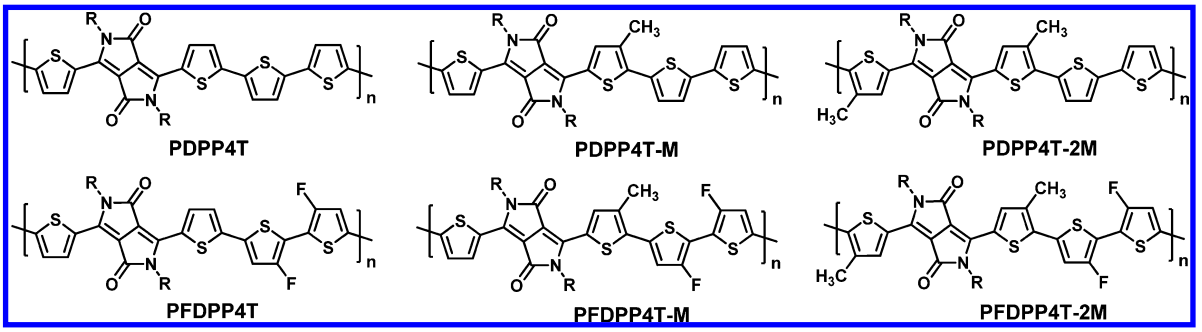

Figure 1. Nonfluorinated and fluorinated DPP polymers studied in this work. PDPP4T-M and PFDPP4T-M have isomeric structures as shown in Figure S2 in the Supporting Information. R is 2′-decyltetradecyl.

Scheme 1. Synthesis of the Monomers and Polymers[a]

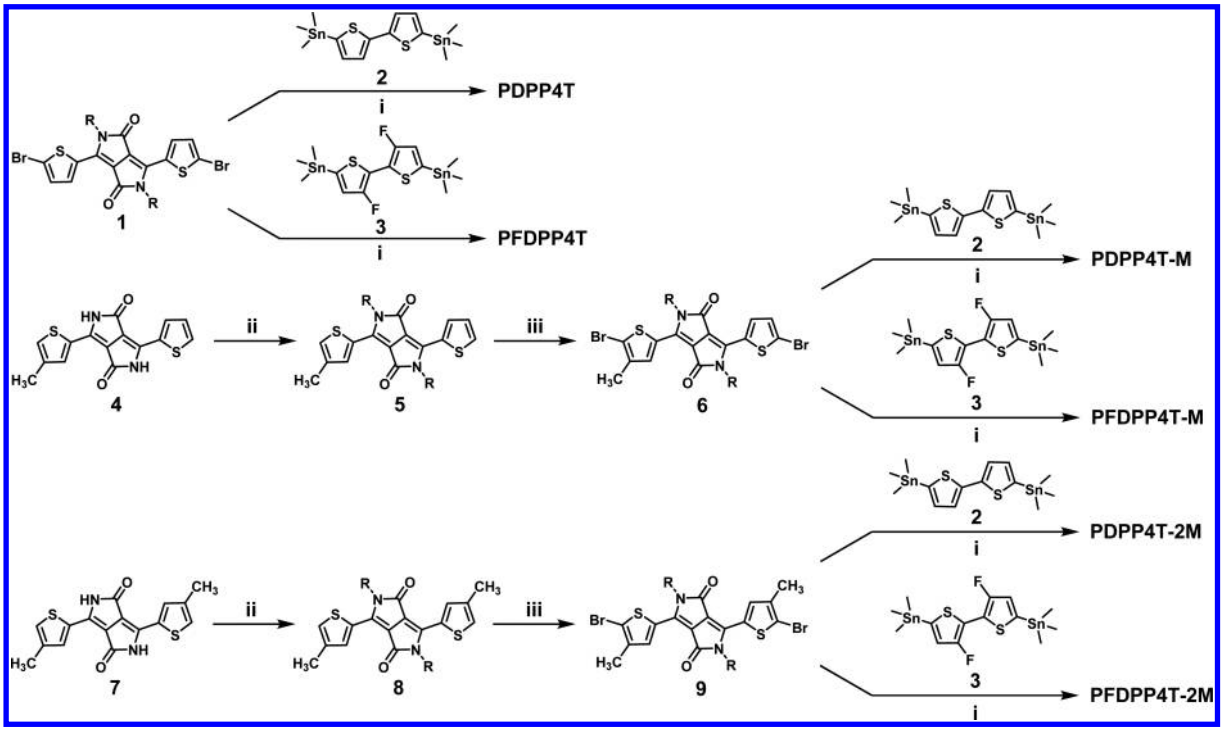

[a]Key: (i) Stille polymerization by using $Pd_2(dba)_3/PPh_3$ in toluene/DMF (10:1, v/v) at 115 °C. (ii) K_2CO_3, 18-crown-6, and 2′-decyltetradecyl bromide in DMF at 120 °C, 16 h. (iii) Br_2/Cs_2CO_3 in $CHCl_3$. R is 2′-decyltetradecyl.

polymers and hence affecting their performance in OFETs. It has been widely reported that, by using the coplanar conjugated backbone[29,39] and the flexible side chains via introducing van der Waals interactions,[32,34,40,41] conjugated polymers can desire good crystal properties. In particular, many reports show that conjugated polymers containing fluorine atoms show enhanced crystallinity with "edge-on" orientation, resulting in high mobilities in OFETs compared to the nonfluorinated polymers (see Figure S1 in Supporting Information).[37,42−48] However, it is also widely reported that fluorinated conjugated polymers usually exhibit high power conversion efficiencies in organic solar cells, which are partially contributed to the enhanced "face-on" orientation of conjugated polymers in thin film.[49−52] The observation in solar cells seems to be inconsistent with the findings in OFETs and therefore will be interesting to provide further investigation.

With these questions, we intentionally introduce fluorine atoms into conjugated backbone, and we wish to systematically study their effect on the microstructure and charge transport of conjugated polymers. As start, we select a highly crystalline diketopyrrolopyrrole (DPP) unit to construct the polymers. The strong electron-deficient DPP units have been widely used to develop conjugated polymers toward high performance FETs.[53,54] Nonfluorinated and fluorinated DPP polymers designed with the same conjugated backbone and alkyl side units (Figure 1) are synthesized and applied into OFETs. Surprisingly, fluorinated polymers show low mobilities below 1.80 $cm^2\ V^{-1}\ s^{-1}$, while nonfluorinated polymers have excellent high mobilities up to 11.16 $cm^2\ V^{-1}\ s^{-1}$. Further investigation by differential scanning calorimetry (DSC) and 2D grazing-incidence wide-angle X-ray scattering (2D-GIWAXS) reveals that fluorinated polymers desire low crystalline properties together with improved "face-on" configuration, explaining their low mobilities in OFETs.

2. RESULTS AND DISCUSSION

Synthesis of the Conjugated Polymers. The synthetic routes for the DPP monomers and polymers are presented in

DOI: 10.1021/acs.macromol.6b01446
Macromolecules XXXX, XXX, XXX−XXX

Table 1. Molecular Weight and Optical and Electrochemical Properties of the Polymers

polymer	M_n (kg mol^{-1})	M_w (kg mol^{-1})	PDI	E_g^{sol} (eV)	E_g^{film} (eV)	HOMO[a] (eV)	LUMO[b] (eV)
PDPP4T	117.1	167.4	1.43	1.43	1.43	−5.34	−3.91
PFDPP4T	116.7	326.6	2.80	1.45	1.42	−5.59	−4.17
PDPP4T-M	64.6	151.0	2.34	1.43	1.44	−5.33	−3.89
PFDPP4T-M	69.8	148.2	2.12	1.46	1.43	−5.46	−4.03
PDPP4T-2M	40.4	90.3	2.23	1.40	1.40	−5.43	−4.03
PFDPP4T-2M	86.1	331.8	3.85	1.41	1.37	−5.43	−4.06

[a]Determined using a work function value of −4.8 eV for Fc/Fc$^+$. [b]Determined as $E_{HOMO} + E_g^{film}$.

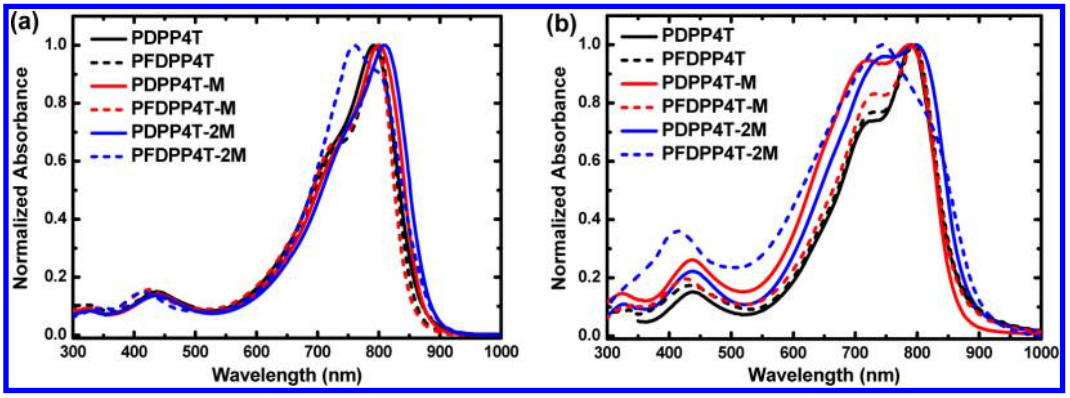

Figure 2. Absorption spectra of DPP polymers (a) in chloroform and (b) in thin films.

Scheme 1 and the detailed synthetic procedures are shown in the Supporting Information. The DPP monomers **1**, **6**, and **9** without or with methyl groups were synthesized according to the literatures.[9,55] The polymers PDPP4T, PDPP4T-M, and PDPP4T-2M were synthesized by Stille polymerization from the dibromo-DPP monomers and 5,5′-bis(trimethylstannyl)-2,2′-bithiophene, in which the catalyst of $Pd_2(dba)_3/PPh_3$ (1:4) and the solvent of toluene/DMF (10:1) were applied. By using the same polymerization condition, the DPP polymers PFDPP4T, PFDPP4T-M and PFDPP4T-2M were synthesized by using the fluorinated bisstannyl-monomer. All these polymers contain the same soluble side chains, 2′-dodecyltetradecyl (DT), to ensure good solubility in $CHCl_3$. It is worth mentioning that, the asymmetric DPP polymers, PDPP4T-M and PFDPP4T-M, also show good solubility in toluene, which is similar to our previous report based on asymmetric structures.[9] The two polymers also have uncertain repeating units, which is owing to the random connection between two monomers, as shown in Figure S2, Supporting Information. The polymers were characterized by gel permeation chromatography (GPC) with *o*-DCB as eluent at 140 °C to determine the molecular weight, as summarized in Table 1. Nonfluorinated polymers PDPP4T, PDPP4T-M and PDPP4T-2M exhibit the number-average molecular weight (M_n) of 117.1 kg mol^{-1}, 64.6 kg mol^{-1} and 40.4 kg mol^{-1}, and fluorinated polymers have similar M_n of 116.7 kg mol^{-1}, 69.8 kg mol^{-1} and 86.1 kg mL^{-1}. The comparable molecular weight is beneficial for the study of charge transports in OFETs.

Absorption Spectra and Energy Levels. All these polymers show similar absorption spectra in thin films with optical bandgaps (E_g) of 1.37−1.43 eV (Figure 2 and Table 1). The absorption shoulder in the small wavelength region can be observed in thin films compared to that in solution, indicating *H*-aggregation of the polymers. The molecular conformation of these DPP polymers was studied by density functional theory (DFT) calculations, revealing the coplanar backbone with small torsion angles (Figure S3, Supporting Information). When incorporating fluorine atoms into the polymers, the torsion angles are significantly reduced, while methyl units show the inverse effect on the dihedral angles. The energy levels of the polymers were determined by cyclic voltammetry in thin films (Figure S4 and Table 1). Fluorinated polymers perform low-lying highest occupied molecular orbital (HOMO) and lowest unoccupied molecular orbital (LUMO) levels due to the electron-withdrawing ability of fluorine atoms.

OFETs. The DPP polymers were applied in OFETs with a bottom gate-bottom contact (BGBC) configuration. The thin films were prepared by spin coating the polymer solution in $CHCl_3$ containing a high boiling point additive *ortho*-dichlorobenzene (*o*-DCB). The thin films were thermal annealed for 10 min under different temperature before measurement. We observe that PDPP4T, PDPP4T-M, PDPP4T-2M, and PFDPP4T-M exhibit the optimized mobility with the thin films annealed at 120 °C, while PFDPP4T and PFDPP4T-2M thin films were thermal annealed at 90 °C to provide the optimized mobilities (Table S1, Supporting Information). The transfer and output characteristics are shown in Figure 3 and Figure S5 in Supporting Information and the charge transport properties are summarized at Table 2.

PDPP4T shows the average hole mobility of 5.67 cm^2 V^{-1} s^{-1}, and the hole mobility is further increased to 9.20 and 9.57 cm^2 V^{-1} s^{-1} for PDPP4T-M and PDPP4T-2M, with the maximum hole mobility of 10.60 and 11.16 cm^2 V^{-1} s^{-1}, respectively. When introducing fluorine atoms into the polymers, the mobilities are dramatically decreased. PFDPP4T shows an average hole mobility of 1.54 cm^2 V^{-1} s^{-1}. After adding one or two methyl units into the polymers, PFDPP4T-M and PFDPP4T-2M presents similar or even low mobilities of 1.53 and 0.81 cm^2 V^{-1} s^{-1} compared to PFDPP4T. The average mobilities were calculated from eight devices (Figure S6, Supporting Information), which also clearly show the trend that nonfluorinated polymers possess much higher mobilities than

DOI: 10.1021/acs.macromol.6b01446
Macromolecules XXXX, XXX, XXX−XXX

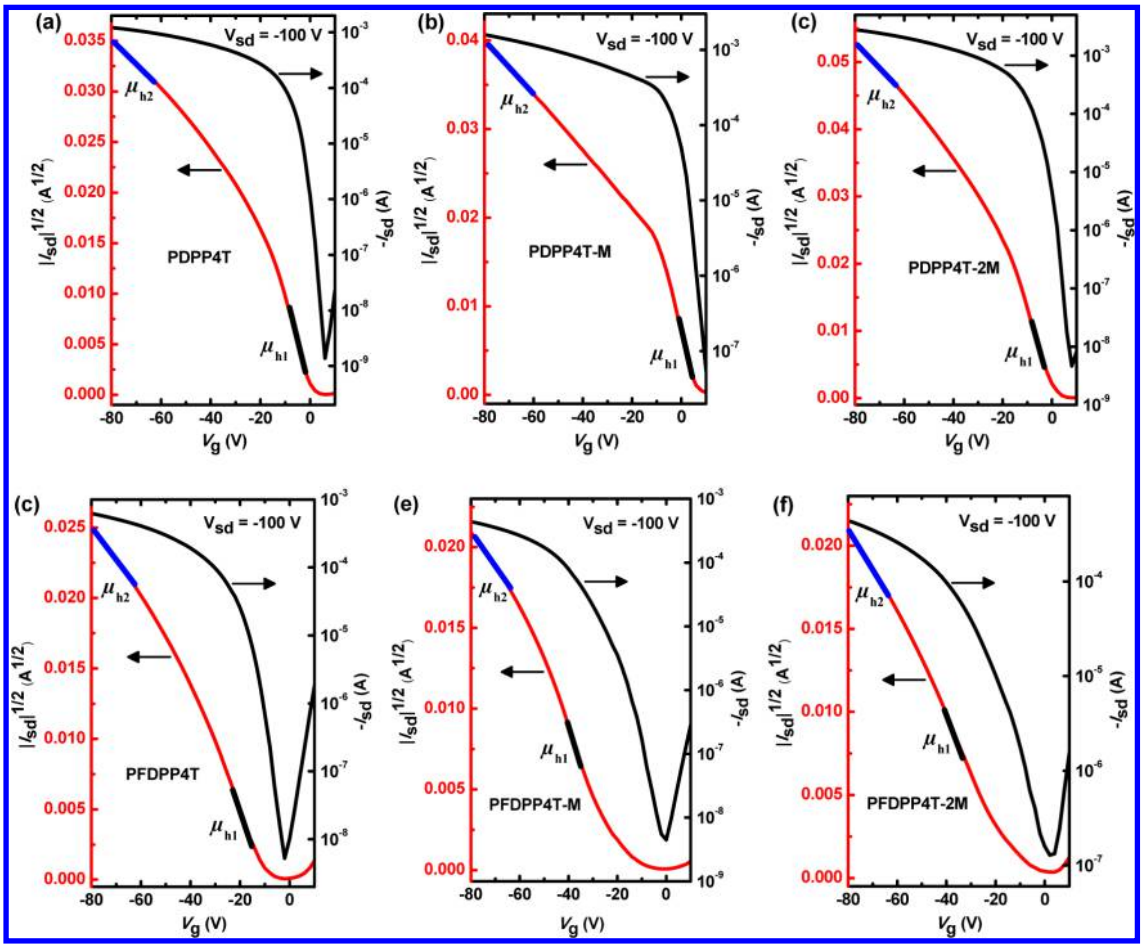

Figure 3. Transfer curves obtained from BGBC FET devices with DPP polymer thin films fabricated from $CHCl_3$ with 10% *o*-DCB. (a) PDPP4T. (b) PDPP4T-M. (c) PDPP4T-2M. (d) PFDPP4T. (e) PFDPP4T-M. (f) PFDPP4T-2M. (c) and (f) Thin films were annealed at 90 °C for 10 min. (a–c and e) Thin films were annealed at 120 °C for 10 min. The hole mobilities are calculated from different gate voltage region: for PDPP4T, μ_{h1} −4 to −10 V; for PDPP4T-M, μ_{h1} +2 to −4 V, for PDPP4T-2M, μ_{h1} −6 to −12 V, for PFDPP4T, μ_{h1} −16 to −22 V; for PFDPP4T-M, μ_{h1} −38 to −44 V, for PFDPP4T-2M, μ_{h1} −36 to −42 V; for all six polymers, μ_{h2} −60 to −80 V.

Table 2. Field-Effect Hole Mobilities of the DPP Polymers in a BGBC Configuration

	μ_{h1} [$cm^2 V^{-1} s^{-1}$]		μ_{h2} [$cm^2 V^{-1} s^{-1}$]		
polymer	av	max	max	V_T [V]	I_{on}/I_{off}
PDPP4T[a]	5.67	6.20	0.38	0.5	1×10^6
PFDPP4T[b]	1.54	1.80	0.35	−10.1	2×10^5
PDPP4T-M[a]	9.20	10.60	0.56	5.7	4×10^4
PFDPP4T-M[a]	1.53	1.66	0.38	−21.7	1×10^5
PDPP4T-2M[a]	9.57	11.16	0.98	0.3	7×10^5
PFDPP4T-2M[b]	0.81	0.91	0.42	−12.4	5×10^3

[a]Thermally annealed at 120 °C. [b]Thermally annealed at 90 °C. The polymer thin films were spin coated from $CHCl_3$/o-DCB (10%).

those of fluorinated DPP polymers. It is also interesting to observe that the DPP polymers containing methyl units desire high hole mobilities in nonfluorinated polymers, but these trends were not observed in fluorinated DPP polymers. We also calculate the hole mobilities (μ_{h2}) over the high gate voltage regime (−60 to −80 V), as suggested in the literature (Figure 3 and Table 2).[56,57] Fluorinated polymers also provided low mobilities compared to those of nonfluorinated polymers, but the distinction between them is narrowed compared to the mobilities calculated from low gate voltage regime.

Morphology and Thermal Analysis. It is desired to further investigate the mobilities difference in these polymers. The morphology of the DPP polymer films were studied by atomic force microscopy (AFM) images, as shown in Figure S7, Supporting Information. Both of nonfluorinated and fluorinated polymers perform similar morphologies with similar surface roughness (0.40–1.07 nm). We then use DSC to study crystal properties of these polymers. Before DSC measurement, we apply thermogravimetric analysis (TGA) to test the stability of the polymers, showing that all the polymers have the good stability with 5% weight loss temperature above 350 °C (Figure S8, Supporting Information). Therefore, we can analyze the thermal transition behavior of the DPP polymers at high temperatures, as shown in Figure 4. All these polymers show melt and crystalline behavior during heating and cooling process, in which nonfluorinated polymers present sharp peaks. The heats of crystallization (ΔH_c) calculated from the DSC thermograms are summarized in Table 3. The polymers PDPP4T, PDPP4T-M, and PDPP4T-2M have ΔH_c of 12.45, 8.37, and 8.28 J g^{-1}. In contrast, fluorinated polymers exhibit the crystal peak with low intensity, as evidenced from the reduced ΔH_c of 5.59, 4.27, and 5.41 J g^{-1} for PFDPP4T, PFDPP4T-M, and PFDPP4T-2M. These measurements indicate that nonfluorinated DPP polymers exhibit high crystalline properties compared to fluorinated DPP polymers.

DOI: 10.1021/acs.macromol.6b01446
Macromolecules XXXX, XXX, XXX–XXX

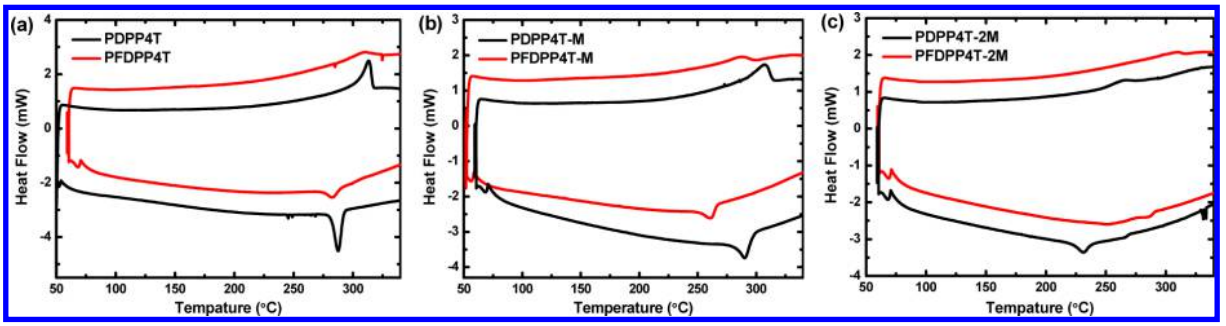

Figure 4. DSC heating and colling traces of the DPP polymers (second cycle) at a scanning speed of 10 °C/min under N_2 (endo up). (a) PDPP4T and PFDPP4T. (b) PDPP4T-M and PFDPP4T-M. (c) PDPP4T-2M and PFDPP4T-2M.

Table 3. Crystallographic Parameters of the Polymer Thin Films[a]

polymer	d(100) [Å]	d(010) [Å]	OOP (010) CL [Å]	IP (010) CL [Å]	T_m (°C)	T_c (°C)	ΔH_c (J g^{-1})
PDPP4T	24.2	3.8	7.1	31.9	313.0	287.4	12.45
PFDPP4T	23.2	3.6	19.1	36.3	307.7	282.6	5.59
PDPP4T-M	22.4	3.9	18.6	31.8	306.7	290.4	8.37
PFDPP4T-M	22.4	3.7	20.5	28.4	286.1	261.4	4.27
PDPP4T-2M	25.1	3.8	–	–	264.7	231.2	8.28
PFDPP4T-2M	26.2	3.9	–	–	306.5	285.9	5.41

[a]The thermal properties of the polymers were also included.

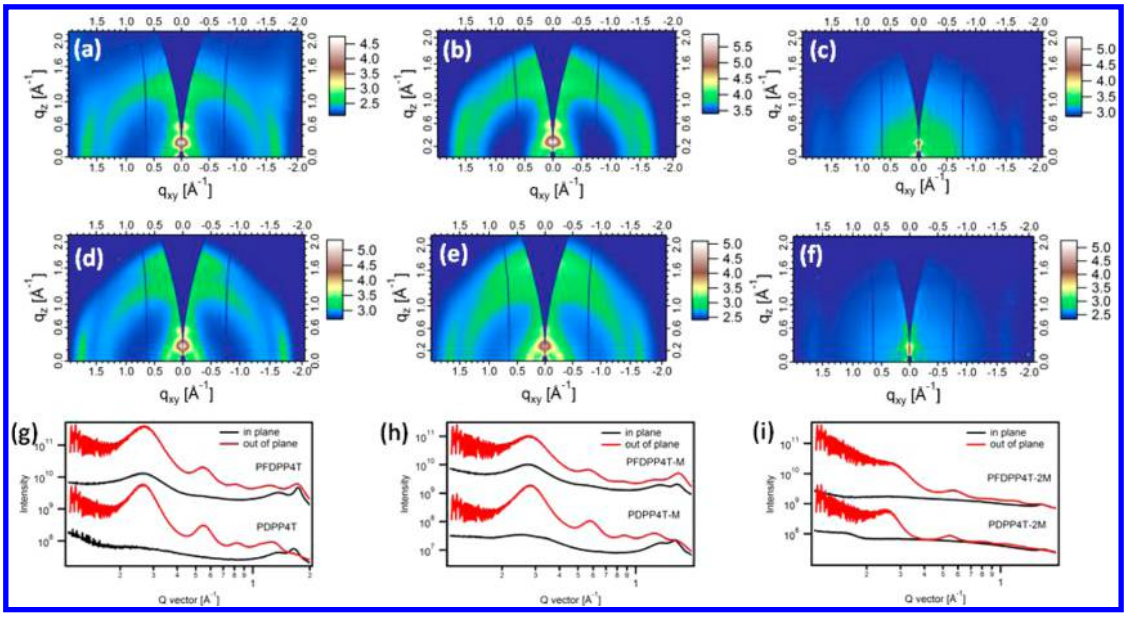

Figure 5. 2D-GIWAXS images of the DPP polymer thin films fabricated from $CHCl_3$ with 10% o-DCB. (a) PDPP4T. (b) PDPP4T-M. (c) PDPP4T-2M. (d) PFDPP4T. (e) PFDPP4T-M. (f) PFDPP4T-2M. (g–i) the OOP and IP cuts of the corresponding 2D-GIWAXS patterns.

GIWAXS Analysis. In order to get insight into the relationship between chemical structures and carrier transport properties, we further applied 2D-GIWAXS to look into the microstructures of the DPP polymers, as shown in Figure 5. At the first glance, we can observe that nonmethylated and asymmetric DPP polymers perform good crystallinity, as evidenced from the series of reflections corresponding to the lamellar packing of the alkyl chains. Distinct (h00) diffraction peaks up to the third order can be observed in the out-of-plane (OOP) direction (Figure 5g–i). (100) peaks of PDPP4T, PDPP4T-M, PFDPP4T, and PFDPP4T-M with the highest intensity at q_z = 0.27, 0.28, 0.26, and 0.28 Å^{-1} correspond to the d-spacings of 2.4, 2.2, 2.3, and 2.2 nm, respectively (Table 3). PDPP4T-2M and PFDPP4T-2M show less crystalline due to weak (100) and (200) diffraction peaks, with similar d-spacings of 2.5 and 2.6 nm from (100) peaks. This demonstrates that the fluorination has little impact on lamellar stacking of alkyl side units.

The orientation of the polymers relative to the substrate can also be obtained from the 2D-GIWAXS patterns and scattering profiles (Figure 5). For nonmethylated and asymmetric DPP polymers, it is clear to show that the introduction of fluorine atoms increases the scattering intensities of the (100) peaks in the in-plane (IP) direction and the (010) peaks in the out-of-plane direction, which indicates that fluorine atoms enhance the proportion of "face-on" orientation. In order to quantitatively analyze this trend, the coherence length (CL) of π–π stacking in the in-plane and the out-of-plane direction for PDPP4T,

DOI: 10.1021/acs.macromol.6b01446
Macromolecules XXXX, XXX, XXX–XXX

PFDPP4T, PDPP4T-M, and PFDPP4T-M are displayed in Table 3. We find that the CL of OOP (010) related to "face-on" orientation is significantly enhanced from 7.1 to19.1 Å for PDPP4T and PFDPP4T, and from 18.6 to20.5 Å for PDPP4T-M and PFDPP4T-M. However, the CL of IP (010) related to "edge-on" orientation slightly changes or shows inverse trend for PDPP4T/PFDPP4T and PDPP4T-M/PFDPP4T-M systems. Consequently, the (010) CL ratio of IP and OOP is 4.5 and 1.7 for PDPP4T and PDPP4T-M, which reduces to 1.9 and 1.4 for PFDPP4T and PFDPP4T-M. This confirms that the number of "face-on" orientated molecules is significantly increased after adding fluorine atoms. Because of the weak (010) peaks of PDPP4T-2M and PFDPP4T-2M, it is difficult to describe the change of the molecular orientation quantitatively, but obviously PFDPP4T-2M shows higher (010) peak in OOP orientation compared with PDPP4T-2M. In brief, the introduction of fluorine atoms leads to an improvement of "face-on" orientation relative to the substrate which is not favorable for the parallel charge transport in FETs, and finally reduce the hole mobility.

It is also interesting to mention that methylated DPP polymer PDPP2T-2M exhibits very low crystalline property (Figure 4c and Figure 5c) but provides the highest hole mobilities among these polymers. The high mobility of PDPP2T-2M may originate from the energetic disorder induced by the rigid conjugated backbone[58] or from the better aggregation in disorder region.[30,31] The intrinsic reason is required to be further investigated.

3. CONCLUSIONS

In conclusion, two series of DPP polymers without or with fluorine atoms were synthesized and applied in OFETs. Fluorinated DPP polymers provide hole mobilities below 1.80 $cm^2\ V^{-1}\ s^{-1}$, while nonfluorinated DPP polymers exhibit high hole mobilities up to 11.16 $cm^2\ V^{-1}\ s^{-1}$, which is also among the highest reported hole mobilities. The low hole mobilities of fluorinated polymers are found to originate from the less crsytallinity and enhanced "face-on" orientation of the polymers. These results demonstrate a very good example that fluorine atoms have detrimental effect on the charge transport in OFETs, which is helpful to understand the relation between chemical structures and charge transport and consequently design new conjugated polymers toward high performance OFETs.

■ ASSOCIATED CONTENT

Supporting Information

The Supporting Information is available free of charge on the ACS Publications website at DOI: 10.1021/acs.macromol.6b01446.

Materials and measurement, synthesis of the monomers and polymers, literature survey of fluorinated polymers for FETs, the chemical structures of PDPP4T-M and PFDPP4T-M, DFT calculations, CV of the polymers, FETs, AFM, and TGA of the DPP polymers, and NMR spectra (PDF)

■ AUTHOR INFORMATION

Corresponding Authors

*(C.L.) E-mail: licheng1987@iccas.ac.cn.
*(Z.W.) E-mail: wangzhaohui@iccas.ac.cn.
*(W.M.) E-mail: msewma@xjtu.edu.cn.
*(W.L.) E-mail: liweiwei@iccas.ac.cn.

Notes

The authors declare no competing financial interest.

■ ACKNOWLEDGMENTS

We thank Qiang Wang and Dr. Ralf Bovee at Eindhoven University of Technology (TU/e, Netherlands) for GPC analysis. This work was supported by the Recruitment Program of Global Youth Experts of China. The work was further supported by the National Natural Science Foundation of China (21574138, 91233205, 21504006, and 21534003) and the Strategic Priority Research Program (XDB12030200) of the Chinese Academy of Sciences. X-ray data was acquired at beamlines 7.3.3 at the Advanced Light Source, which is supported by the Director, Office of Science, Office of Basic Energy Sciences, of the U.S. Department of Energy, under Contract No. DE-AC02-05CH11231.

■ REFERENCES

(1) Sirringhaus, H. 25th Anniversary Article: Organic Field-Effect Transistors: The Path Beyond Amorphous Silicon. *Adv. Mater.* **2014**, *26*, 1319−1335.

(2) Yan, H.; Chen, Z.; Zheng, Y.; Newman, C.; Quinn, J. R.; Dotz, F.; Kastler, M.; Facchetti, A. A high-mobility electron-transporting polymer for printed transistors. *Nature* **2009**, *457*, 679−686.

(3) Sekitani, T.; Zschieschang, U.; Klauk, H.; Someya, T. Flexible organic transistors and circuits with extreme bending stability. *Nat. Mater.* **2010**, *9*, 1015−1022.

(4) Li, J.; Zhao, Y.; Tan, H. S.; Guo, Y.; Di, C.-A.; Yu, G.; Liu, Y.; Lin, M.; Lim, S. H.; Zhou, Y.; Su, H.; Ong, B. S. A stable solution-processed polymer semiconductor with record high-mobility for printed transistors. *Sci. Rep.* **2012**, *2*, 754.

(5) Benight, S. J.; Wang, C.; Tok, J. B. H.; Bao, Z. Stretchable and self-healing polymers and devices for electronic skin. *Prog. Polym. Sci.* **2013**, *38*, 1961−1977.

(6) Zang, Y.; Zhang, F.; Huang, D.; Gao, X.; Di, C.-a.; Zhu, D. Flexible suspended gate organic thin-film transistors for ultra-sensitive pressure detection. *Nat. Commun.* **2015**, *6*, 6269.

(7) Bucella, S. G.; Luzio, A.; Gann, E.; Thomsen, L.; McNeill, C. R.; Pace, G.; Perinot, A.; Chen, Z.; Facchetti, A.; Caironi, M. Macroscopic and high-throughput printing of aligned nanostructured polymer semiconductors for MHz large-area electronics. *Nat. Commun.* **2015**, *6*, 8394.

(8) Baeg, K.-J.; Caironi, M.; Noh, Y.-Y. Toward Printed Integrated Circuits based on Unipolar or Ambipolar Polymer Semiconductors. *Adv. Mater.* **2013**, *25*, 4210−4244.

(9) Ji, Y.; Xiao, C.; Wang, Q.; Zhang, J.; Li, C.; Wu, Y.; Wei, Z.; Zhan, X.; Hu, W.; Wang, Z.; Janssen, R. A. J.; Li, W. Asymmetric Diketopyrrolopyrrole Conjugated Polymers for Field-Effect Transistors and Polymer Solar Cells Processed from a Nonchlorinated Solvent. *Adv. Mater.* **2016**, *28*, 943−950.

(10) Back, J. Y.; Yu, H.; Song, I.; Kang, I.; Ahn, H.; Shin, T. J.; Kwon, S.-K.; Oh, J. H.; Kim, Y.-H. Investigation of Structure−Property Relationships in Diketopyrrolopyrrole-Based Polymer Semiconductors via Side-Chain Engineering. *Chem. Mater.* **2015**, *27*, 1732−1739.

(11) Tseng, H.-R.; Phan, H.; Luo, C.; Wang, M.; Perez, L. A.; Patel, S. N.; Ying, L.; Kramer, E. J.; Nguyen, T.-Q.; Bazan, G. C.; Heeger, A. J. High-Mobility Field-Effect Transistors Fabricated with Macroscopic Aligned Semiconducting Polymers. *Adv. Mater.* **2014**, *26*, 2993−2998.

(12) Kim, G.; Kang, S.-J.; Dutta, G. K.; Han, Y.-K.; Shin, T. J.; Noh, Y.-Y.; Yang, C. A Thienoisoindigo-Naphthalene Polymer with Ultrahigh Mobility of 14.4 cm2/V·s That Substantially Exceeds Benchmark Values for Amorphous Silicon Semiconductors. *J. Am. Chem. Soc.* **2014**, *136*, 9477−9483.

(13) Nketia-Yawson, B.; Lee, H. S.; Seo, D.; Yoon, Y.; Park, W. T.; Kwak, K.; Son, H. J.; Kim, B.; Noh, Y. Y. A Highly Planar Fluorinated

DOI: 10.1021/acs.macromol.6b01446
Macromolecules XXXX, XXX, XXX−XXX

Benzothiadiazole-Based Conjugated Polymer for High-Performance Organic Thin-Film Transistors. *Adv. Mater.* **2015**, *27*, 3045−3052.
(14) Kang, B.; Kim, R.; Lee, S. B.; Kwon, S.-K.; Kim, Y.-H.; Cho, K. Side-Chain-Induced Rigid Backbone Organization of Polymer Semiconductors through Semifluoroalkyl Side Chains. *J. Am. Chem. Soc.* **2016**, *138*, 3679−3686.
(15) Sung, M. J.; Luzio, A.; Park, W.-T.; Kim, R.; Gann, E.; Maddalena, F.; Pace, G.; Xu, Y.; Natali, D.; de Falco, C.; Dang, L.; McNeill, C. R.; Caironi, M.; Noh, Y.-Y.; Kim, Y.-H. High-Mobility Naphthalene Diimide and Selenophene-Vinylene-Selenophene-Based Conjugated Polymer: n-Channel Organic Field-Effect Transistors and Structure−Property Relationship. *Adv. Funct. Mater.* **2016**, *26*, 4984−4997.
(16) Zheng, Y.-Q.; Lei, T.; Dou, J.-H.; Xia, X.; Wang, J.-Y.; Liu, C.-J.; Pei, J. Strong Electron-Deficient Polymers Lead to High Electron Mobility in Air and Their Morphology-Dependent Transport Behaviors. *Adv. Mater.* **2016**, DOI: 10.1002/adma.201600541.
(17) Li, H.; Kim, F. S.; Ren, G.; Jenekhe, S. A. High-Mobility n-Type Conjugated Polymers Based on Electron-Deficient Tetraazabenzodifluoranthene Diimide for Organic Electronics. *J. Am. Chem. Soc.* **2013**, *135*, 14920−14923.
(18) Durban, M. M.; Kazarinoff, P. D.; Luscombe, C. K. Synthesis and Characterization of Thiophene-Containing Naphthalene Diimide n-Type Copolymers for OFET Applications. *Macromolecules* **2010**, *43*, 6348−6352.
(19) Yun, H.-J.; Kang, S.-J.; Xu, Y.; Kim, S. O.; Kim, Y.-H.; Noh, Y.-Y.; Kwon, S.-K. Dramatic Inversion of Charge Polarity in Diketopyrrolopyrrole-Based Organic Field-Effect Transistors via a Simple Nitrile Group Substitution. *Adv. Mater.* **2014**, *26*, 7300−7307.
(20) Sun, B.; Hong, W.; Yan, Z.; Aziz, H.; Li, Y. Record High Electron Mobility of 6.3 cm2V−1s−1 Achieved for Polymer Semiconductors Using a New Building Block. *Adv. Mater.* **2014**, *26*, 2636−2642.
(21) Khim, D.; Cheon, Y. R.; Xu, Y.; Park, W.-T.; Kwon, S.-K.; Noh, Y.-Y.; Kim, Y.-H. Facile Route To Control the Ambipolar Transport in Semiconducting Polymers. *Chem. Mater.* **2016**, *28*, 2287−2294.
(22) Lee, J.; Han, A. R.; Yu, H.; Shin, T. J.; Yang, C.; Oh, J. H. Boosting the Ambipolar Performance of Solution-Processable Polymer Semiconductors via Hybrid Side-Chain Engineering. *J. Am. Chem. Soc.* **2013**, *135*, 9540−9547.
(23) Sun, B.; Hong, W.; Aziz, H.; Li, Y. A pyridine-flanked diketopyrrolopyrrole (DPP)-based donor-acceptor polymer showing high mobility in ambipolar and n-channel organic thin film transistors. *Polym. Chem.* **2015**, *6*, 938−945.
(24) Sirringhaus, H.; Brown, P. J.; Friend, R. H.; Nielsen, M. M.; Bechgaard, K.; Langeveld-Voss, B. M. W.; Spiering, A. J. H.; Janssen, R. A. J.; Meijer, E. W.; Herwig, P.; de Leeuw, D. M. Two-dimensional charge transport in self-organized, high-mobility conjugated polymers. *Nature* **1999**, *401*, 685−688.
(25) McCulloch, I.; Heeney, M.; Bailey, C.; Genevicius, K.; MacDonald, I.; Shkunov, M.; Sparrowe, D.; Tierney, S.; Wagner, R.; Zhang, W. M.; Chabinyc, M. L.; Kline, R. J.; Mcgehee, M. D.; Toney, M. F. Liquid-crystalline semiconducting polymers with high charge-carrier mobility. *Nat. Mater.* **2006**, *5*, 328−333.
(26) DeLongchamp, D. M.; Kline, R. J.; Lin, E. K.; Fischer, D. A.; Richter, L. J.; Lucas, L. A.; Heeney, M.; McCulloch, I.; Northrup, J. E. High carrier mobility polythiophene thin films: Structure determination by experiment and theory. *Adv. Mater.* **2007**, *19*, 833−837.
(27) Facchetti, A. π-Conjugated Polymers for Organic Electronics and Photovoltaic Cell Applications. *Chem. Mater.* **2011**, *23*, 733−758.
(28) Zhang, W.; Smith, J.; Watkins, S. E.; Gysel, R.; McGehee, M.; Salleo, A.; Kirkpatrick, J.; Ashraf, S.; Anthopoulos, T.; Heeney, M.; McCulloch, I. Indacenodithiophene Semiconducting Polymers for High-Performance, Air-Stable Transistors. *J. Am. Chem. Soc.* **2010**, *132*, 11437−11439.
(29) Zhang, W.; Han, Y.; Zhu, X.; Fei, Z.; Feng, Y.; Treat, N. D.; Faber, H.; Stingelin, N.; McCulloch, I.; Anthopoulos, T. D.; Heeney, M. A Novel Alkylated Indacenodithieno[3,2-b]thiophene-Based Polymer for High-Performance Field-Effect Transistors. *Adv. Mater.* **2016**, *28*, 3922−3927.
(30) Noriega, R.; Rivnay, J.; Vandewal, K.; Koch, F. P. V.; Stingelin, N.; Smith, P.; Toney, M. F.; Salleo, A. A general relationship between disorder, aggregation and charge transport in conjugated polymers. *Nat. Mater.* **2013**, *12*, 1038−1044.
(31) Zhang, X.; Bronstein, H.; Kronemeijer, A. J.; Smith, J.; Kim, Y.; Kline, R. J.; Richter, L. J.; Anthopoulos, T. D.; Sirringhaus, H.; Song, K.; Heeney, M.; Zhang, W.; McCulloch, I.; DeLongchamp, D. M. Molecular origin of high field-effect mobility in an indacenodithiophene−benzothiadiazole copolymer. *Nat. Commun.* **2013**, *4*, 2238.
(32) Han, A. R.; Dutta, G. K.; Lee, J.; Lee, H. R.; Lee, S. M.; Ahn, H.; Shin, T. J.; Oh, J. H.; Yang, C. ε-Branched Flexible Side Chain Substituted Diketopyrrolopyrrole-Containing Polymers Designed for High Hole and Electron Mobilities. *Adv. Funct. Mater.* **2015**, *25*, 247−254.
(33) Lei, T.; Dou, J.-H.; Cao, X.-Y.; Wang, J.-Y.; Pei, J. A BDOPV-Based Donor−Acceptor Polymer for High-Performance n-Type and Oxygen-Doped Ambipolar Field-Effect Transistors. *Adv. Mater.* **2013**, *25*, 6589−6593.
(34) Kang, I.; Yun, H.-J.; Chung, D. S.; Kwon, S.-K.; Kim, Y.-H. Record High Hole Mobility in Polymer Semiconductors via Side-Chain Engineering. *J. Am. Chem. Soc.* **2013**, *135*, 14896−14899.
(35) Rivnay, J.; Toney, M. F.; Zheng, Y.; Kauvar, I. V.; Chen, Z. H.; Wagner, V.; Facchetti, A.; Salleo, A. Unconventional Face-On Texture and Exceptional In-Plane Order of a High Mobility n-Type Polymer. *Adv. Mater.* **2010**, *22*, 4359−4363.
(36) Mei, J.; Kim, D. H.; Ayzner, A. L.; Toney, M. F.; Bao, Z. Siloxane-Terminated Solubilizing Side Chains: Bringing Conjugated Polymer Backbones Closer and Boosting Hole Mobilities in Thin-Film Transistors. *J. Am. Chem. Soc.* **2011**, *133*, 20130−20133.
(37) Park, J. H.; Jung, E. H.; Jung, J. W.; Jo, W. H. A Fluorinated Phenylene Unit as a Building Block for High-Performance n-Type Semiconducting Polymer. *Adv. Mater.* **2013**, *25*, 2583−2588.
(38) Xiao, C.; Zhao, G.; Zhang, A.; Jiang, W.; Janssen, R. A. J.; Li, W.; Hu, W.; Wang, Z. High Performance Polymer Nanowire Field-Effect Transistors with Distinct Molecular Orientations. *Adv. Mater.* **2015**, *27*, 4963−4968.
(39) Chen, H.; Guo, Y.; Yu, G.; Zhao, Y.; Zhang, J.; Gao, D.; Liu, H.; Liu, Y. Highly π-Extended Copolymers with Diketopyrrolopyrrole Moieties for High-Performance Field-Effect Transistors. *Adv. Mater.* **2012**, *24*, 4618−4622.
(40) Yao, J.; Yu, C.; Liu, Z.; Luo, H.; Yang, Y.; Zhang, G.; Zhang, D. Significant Improvement of Semiconducting Performance of the Diketopyrrolopyrrole−Quaterthiophene Conjugated Polymer through Side-Chain Engineering via Hydrogen-Bonding. *J. Am. Chem. Soc.* **2016**, *138*, 173−185.
(41) Lei, T.; Dou, J.-H.; Pei, J. Influence of Alkyl Chain Branching Positions on the Hole Mobilities of Polymer Thin-Film Transistors. *Adv. Mater.* **2012**, *24*, 6457−6461.
(42) Fei, Z.; Boufflet, P.; Wood, S.; Wade, J.; Moriarty, J.; Gann, E.; Ratcliff, E. L.; McNeill, C. R.; Sirringhaus, H.; Kim, J.-S.; Heeney, M. Influence of Backbone Fluorination in Regioregular Poly(3-alkyl-4-fluoro)thiophenes. *J. Am. Chem. Soc.* **2015**, *137*, 6866−6879.
(43) Boufflet, P.; Han, Y.; Fei, Z.; Treat, N. D.; Li, R.; Smilgies, D.-M.; Stingelin, N.; Anthopoulos, T. D.; Heeney, M. Using Molecular Design to Increase Hole Transport: Backbone Fluorination in the Benchmark Material Poly(2,5-bis(3-alkylthiophen-2-yl)thieno[3,2-b]-thiophene (pBTTT). *Adv. Funct. Mater.* **2015**, *25*, 7038−7048.
(44) Kim, H. G.; Kang, B.; Ko, H.; Lee, J.; Shin, J.; Cho, K. Synthetic Tailoring of Solid-State Order in Diketopyrrolopyrrole-Based Copolymers via Intramolecular Noncovalent Interactions. *Chem. Mater.* **2015**, *27*, 829−838.
(45) Lei, T.; Xia, X.; Wang, J.-Y.; Liu, C.-J.; Pei, J. Conformation Locked" Strong Electron-Deficient Poly(p-Phenylene Vinylene) Derivatives for Ambient-Stable n-Type Field-Effect Transistors: Synthesis, Properties, and Effects of Fluorine Substitution Position. *J. Am. Chem. Soc.* **2014**, *136*, 2135−2141.

DOI: 10.1021/acs.macromol.6b01446
Macromolecules XXXX, XXX, XXX−XXX

(46) Wang, X.; Zhang, Z.-G.; Luo, H.; Chen, S.; Yu, S.; Wang, H.; Li, X.; Yu, G.; Li, Y. Effects of fluorination on the properties of thieno[3,2-b]thiophene-bridged donor-[small pi]-acceptor polymer semiconductors. *Polym. Chem.* **2014**, *5*, 502−511.
(47) Yum, S.; An, T. K.; Wang, X.; Lee, W.; Uddin, M. A.; Kim, Y. J.; Nguyen, T. L.; Xu, S.; Hwang, S.; Park, C. E.; Woo, H. Y. Benzotriazole-Containing Planar Conjugated Polymers with Non-covalent Conformational Locks for Thermally Stable and Efficient Polymer Field-Effect Transistors. *Chem. Mater.* **2014**, *26*, 2147−2154.
(48) Lei, T.; Dou, J.-H.; Ma, Z.-J.; Yao, C.-H.; Liu, C.-J.; Wang, J.-Y.; Pei, J. Ambipolar Polymer Field-Effect Transistors Based on Fluorinated Isoindigo: High Performance and Improved Ambient Stability. *J. Am. Chem. Soc.* **2012**, *134*, 20025−20028.
(49) Leclerc, N.; Chávez, P.; Ibraikulov, O.; Heiser, T.; Lévêque, P. Impact of Backbone Fluorination on π-Conjugated Polymers in Organic Photovoltaic Devices: A Review. *Polymers* **2016**, *8*, 11.
(50) Liu, Y.; Zhao, J.; Li, Z.; Mu, C.; Ma, W.; Hu, H.; Jiang, K.; Lin, H.; Ade, H.; Yan, H. Aggregation and morphology control enables multiple cases of high-efficiency polymer solar cells. *Nat. Commun.* **2014**, *5*, 5293.
(51) Vohra, V.; Kawashima, K.; Kakara, T.; Koganezawa, T.; Osaka, I.; Takimiya, K.; Murata, H. Efficient inverted polymer solar cells employing favourable molecular orientation. *Nat. Photonics* **2015**, *9*, 403−408.
(52) Chen, H. Y.; Hou, J. H.; Zhang, S. Q.; Liang, Y. Y.; Yang, G. W.; Yang, Y.; Yu, L. P.; Wu, Y.; Li, G. polymer solar cells with enhanced open-circuit voltage and efficiency. *Nat. Photonics* **2009**, *3*, 649.
(53) Yi, Z.; Wang, S.; Liu, Y. Design of High-Mobility Diketopyrrolopyrrole-Based π-Conjugated Copolymers for Organic Thin-Film Transistors. *Adv. Mater.* **2015**, *27*, 3589−3606.
(54) Nielsen, C. B.; Turbiez, M.; McCulloch, I. Recent Advances in the Development of Semiconducting DPP-Containing Polymers for Transistor Applications. *Adv. Mater.* **2013**, *25*, 1859−1880.
(55) Li, W.; Furlan, A.; Hendriks, K. H.; Wienk, M. M.; Janssen, R. A. J. Efficient Tandem and Triple-Junction Polymer Solar Cells. *J. Am. Chem. Soc.* **2013**, *135*, 5529−5532.
(56) McCulloch, I.; Salleo, A.; Chabinyc, M. Avoid the kinks when measuring mobility. *Science* **2016**, *352*, 1521−1522.
(57) Bittle, E. G.; Basham, J. I.; Jackson, T. N.; Jurchescu, O. D.; Gundlach, D. J. Mobility overestimation due to gated contacts in organic field-effect transistors. *Nat. Commun.* **2016**, *7*, 10908.
(58) Venkateshvaran, D.; Nikolka, M.; Sadhanala, A.; Lemaur, V.; Zelazny, M.; Kepa, M.; Hurhangee, M.; Kronemeijer, A. J.; Pecunia, V.; Nasrallah, I.; Romanov, I.; Broch, K.; McCulloch, I.; Emin, D.; Olivier, Y.; Cornil, J.; Beljonne, D.; Sirringhaus, H. Approaching disorder-free transport in high-mobility conjugated polymers. *Nature* **2014**, *515*, 384−388.

DOI: 10.1021/acs.macromol.6b01446
Macromolecules XXXX, XXX, XXX−XXX